Journal of Applied Polymer Science

Morphology and toughness enhancements in recycled high-density polyethylene (rHDPE) via solid-state shear pulverization (SSSP) and solid-state/melt extrusion (SSME)

Evan V. Miu, Andrew J. Fox, Samuel H. Jubb, Katsuyuki Wakabayashi
Department of Chemical Engineering, Bucknell University, Lewisburg, Pennsylvania 17837, U. S. A.
Correspondence to: K. Wakabayashi (E-mail: kat.wakabayashi@bucknell.edu)

ABSTRACT: Solid-state, mechanochemical polymer processing techniques are explored as an effective and sustainable solution to appearance and performance issues commonly associated with recycled plastic products. Post-consumer high-density polyethylene (HDPE) from milk jugs is processed via conventional twin screw extrusion (TSE), solid-state shear pulverization (SSSP), and solid-state/melt extrusion (SSME), and compared to the as-received and virgin forms regarding output attributes and mechanical properties, as well as morphology. Solid-state processing methods, particularly SSME with a harsh screw configuration, produce samples with consistent appearance and melt flow characteristics. Tensile ductility/toughness and impact toughness are enhanced by up to 11-fold as compared to the as-received sample, to a level near and above those of an equivalent virgin HDPE. Calorimetry, optical microscopy, X-ray scattering, and rheology characterization reveal that the mechanical improvements result from a favorable combination of physical and molecular changes in rHDPE, such as impurity size reduction, spherulite size enlargement, and chain branching. © 2015 Wiley Periodicals, Inc. J. Appl. Polym. Sci. **2016**, *133*, 43070.

KEYWORDS: compatibilization; extrusion; mechanical properties; recycling; thermoplastics

Received 28 August 2015; accepted 16 October 2015
DOI: 10.1002/app.43070

INTRODUCTION

As thermoplastics continue to be applicable in a vast range of products for numerous practical and economic reasons, they contribute to consumer waste throughout the world. Since its inception over three decades ago, plastics recycling has evolved into a more diverse resource recovery means, with such different types as mechanical, thermal, and chemical recycling.[1–3] Growing public interest and research efforts indicate that plastics recycling is still at the heart of today's sustainability focus.

High-density polyethylene (HDPE) accounts for the highest tonnage production of all plastic types in North America today,[4] and the material is prominently found in the consumer market as disposable bags and containers (e.g., plastic milk jugs).[5,6] Even though post-consumer HDPEs are relatively well-collected and -recycled through curbside and retail store programming, the total recovery rate for HDPE is just above 10%,[7] while HDPE bottles are recovered at a higher rate of 32%.[8] As the growing commercial demand for HDPE extends beyond packaging—to barrier, piping, lumber, and sports and leisure applications[5,6]—significant opportunities exist for mechanically-recycled HDPEs (rHDPEs) to replace conventional virgin HDPEs (vHDPEs).

Even with the advantage that the market price of rHDPE is lower than that of vHDPE, the use of rHDPEs in the manufacturing industry is limited to mostly downcycling[9] into low value, low risk products, such as rubbish bins, detergent bottles, crates, and pallets.[8] The major reason for the discrepancy between availability and usability of rHDPEs is their marked deterioration in properties and performance when compared to the virgin forms. Reprocessing of rHDPE in extreme conditions and repetitions often results in the alteration of their macromolecular structure via chain scission and branching,[10–14] though several reports indicate that normal reprocessing in the form of mechanical recycling does not necessarily alter the typical use-temperature performance of HDPE to a significant extent.[13,15–17] Moreover, manufacturers suffer from batch-to-batch variation in rHDPE feedstock as a result of differing original vHDPE grades and inherent impurities from imperfect recovering and sorting techniques.[3] The more serious disadvantages of rHDPEs are practical issues like inconsistent processing characteristics (e.g., viscosity, melt-strength) and output product quality (color, physical properties).

Numerous efforts have been made to compensate for the inferior properties of rHDPE, via use as a filler in structural materials[18–20] and as a component in blends with vHDPEs[21–23] or

other polymers.[23–25] Similarly, rHDPEs have been reinforced with natural fibers,[26–31] minerals,[32–34] and ground tire particles[35–37] and marketed as green composites. While these cases effectively utilize rHDPE, the implementation is often haphazard and forced, without accounting for the technical value of rHDPE in the corresponding products. Other efforts include developing chemical routes to transform rHDPE into more industrially relevant grades. Manipulating the rHDPE chain structure with small molecule additives (e.g., stabilizers, chain extenders, crosslinking agents) have led to more mechanically robust rHDPEs,[38–40] and certain chemical binders can force rHDPE to be more compatible with other materials.[27,41,42] Although promising, these methodologies require use of complex—and often publicly unknown and proprietary—chemicals, which render them less environmentally friendly, and thus not as sustainable as originally intended.

A method for genuine, direct, and truly sustainable mechanical recycling of HDPE into self-sufficient rHDPE-applications would be beneficial. Solid-state shear pulverization (SSSP) is an alternative, low-temperature processing technique derived from industrial plastics extrusion, originally targeted for size reduction and mixing of post-consumer rubber and plastic particles.[43,44] Recent reports have showcased that the capabilities of SSSP have expanded into fabrication of value-added polymer products in a commercially scalable, environmentally benign fashion. SSSP, along with its revised version of solid-state/melt extrusion (SSME), has been reported to fabricate various homopolymers,[45,46] polymer blends,[47,48] and polymer composites[49,50] and nanocomposites[51–53] with enhanced morphologies and physical properties. The successes of these fabricated products rely on the unique feature inherent to the SSSP and SSME processes of solid-state mechanochemistry through continuous high shear and compressive forces in the chilled extruder setup. In the present article, the same SSSP and SSME principles are exploited in post-consumer HDPE from milk jugs, a model recycled plastic material. The investigation focuses on the improvements in processing characteristics and product consistency, as well as the structure-property relationships of the resulting materials in comparison with conventional reprocessing methods.

EXPERIMENTAL

Materials

Post-consumer, recycled high density polyethylene (rHDPE) from milk jugs was kindly provided by Waste Not Technologies, LLC (Saylorsburg, PA). The milk jugs were granulated, washed in an agitated water bath at 70°C, and sent through a heated air dryer. Potential contaminants in a postconsumer collection include printed paper and polypropylene (PP) films from the labels, pigmented injection-molding grade HDPE from screw-style caps, and pigmented injection-molding grade low-density polyethylene (LDPE) from snap-style caps. The washing system removed most of these impurities from granulated rHDPE milk jug flakes, but low, inconsistent levels of non-HDPE materials remained in the batch. These as-received rHDPE flakes were the only material used in processing; no stabilizers, compatibilizers, or processing aids were added. As a point of comparison, commercial, blow-molding/milk jug grade, virgin HDPE (vHDPE) from LyondellBasell (reported MFI = 0.8 g/10 min and $\rho = 0.96$ g cm^{-3}) was acquired and tested along with the unprocessed and processed rHDPE.

Processing

A KrausMaffei Berstorff ZE-25 UTX twin screw extruder, which has intermeshing, corotating, 25-mm diameter screws, was employed for twin screw melt extrusion (TSE), solid state shear pulverization (SSSP), and solid state melt extrusion (SSME) processes. Figure 1 presents the custom temperature controls and screw configurations that were specified for the TSE, SSSP, and SSME processes. The solid state processing zones were chilled by the coolant channels residing very close to the barrel walls, through which a continuous flow of ethylene glycol-water solution at −12°C was supplied by a Budzar Industries BWA-AC10 chiller. The melt state processing zones were heated with cartridge-type electrical heaters. The screw configurations were designed with spiral conveying and bilobe kneading elements arranged in intermittent series, as shown in Figure 1. The TSE processing was conducted with one standard commercial screw design set-up, while SSSP and SSME processing each used two custom screw configurations arranged for mild (low) and harsh (high) shear/compression settings; the corresponding specimens are named with the "-L" and "-H" suffixes, respectively. For consistency, all the processes used the identical screw rotation speed at 200 rpm, and the same throughput, at 200 g h^{-1}; the raw material was metered using a Brabender Technologie DS28-10 screw feeder. The SSME and TSE processes yielded continuous molten extrudate through a standard three-hole extrusion die, which was cooled and pelletized using a Scheer Bay BT-25 system. The SSSP process yielded a powder output, which fell out of an endcap zone open to the atmosphere. Further information about the SSSP and SSME instrumentation is available in previous reports.[45,47,53]

Characterization

Processed and control samples were compression-molded into 0.5-mm thick sheets using a Carver Model C Laboratory Press operating at 200°C. The sheets were subsequently air-cooled to room temperature, and stored at room temperature for at least 24 h prior to any testing. For uniaxial tensile testing according to ASTM D1708, tensile coupons were cut using a Dewes-Gumbs 1.5T DGD expulsion system. An elongation rate of 1.27 cm min^{-1} was used to test the specimens in Tinius-Olsen H5K-S, and the resulting stress-strain data were analyzed using an in-house-developed software program. Impact resistance test followed ASTM D4812. Samples were injection-molded into 12.7 × 63.5 × 3.17 mm^3 slabs using an AB Plastics Model 200 injection molder operating at 200°C and 400 kPa ram pressure. A Tinius-Olsen Model IT504 pendulum system recorded the absorbed energy.

For thermal characterization, small specimens of 5–7 mg were punched from the compression-molded sheets and analyzed in a TA Instruments Q1000 differential scanning calorimeter (DSC). For the determination of the melting and crystallization temperatures and enthalpies, a heat/cool 10°C min^{-1} ramp mode was set between −40 and 240°C. Polyethylene crystallinity

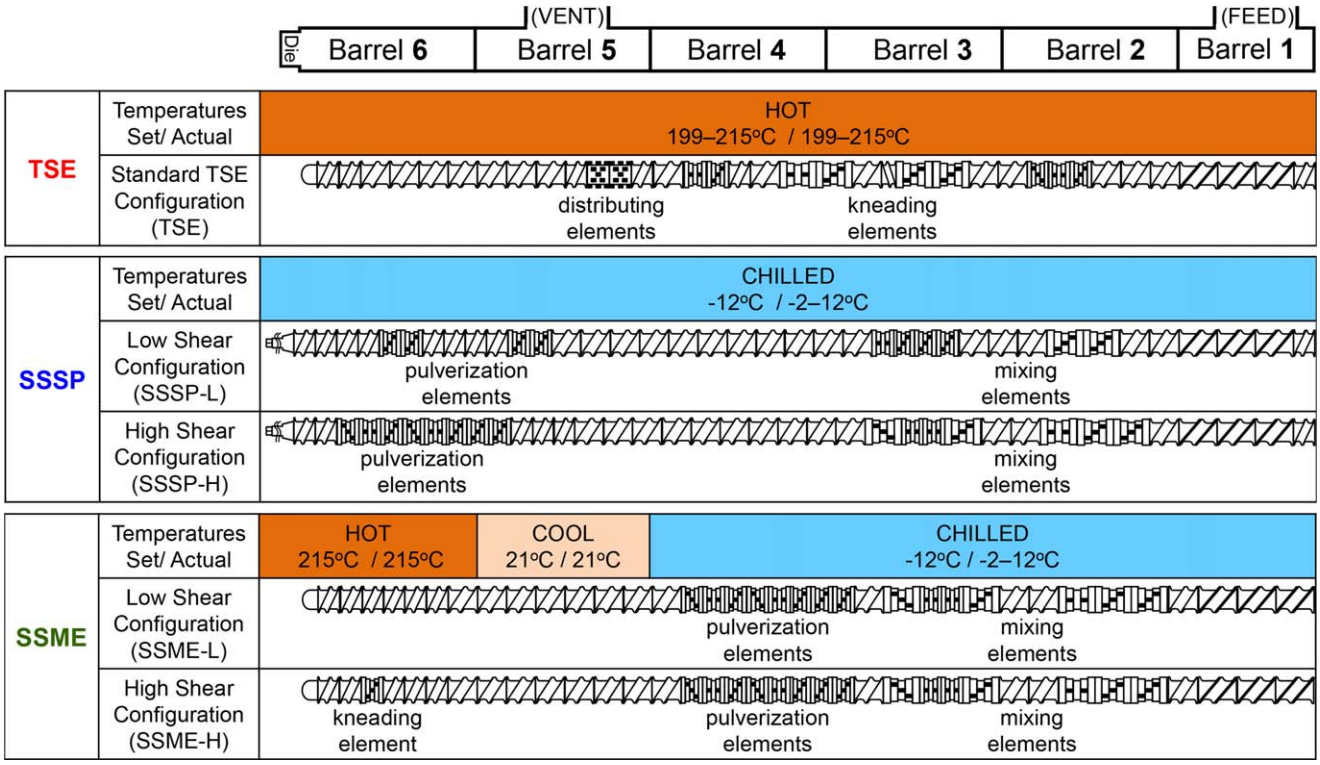

Figure 1. Barrel and screw configurations for the three different methods of processing. Screw elements are either of the spiral conveying or bilobe kneading/mixing/pulverization types. *L*/*D* ratio for TSE and SSME is 34, and that for SSSP is 36. [Color figure can be viewed in the online issue, which is available at wileyonlinelibrary.com.]

was determined by dividing the latent heat of melting by that of a theoretically 100% crystalline polyethylene, 293 J g^{-1}.[54] For the determination of the crystallization kinetics, an isothermal method heated the specimens to 240°C at a rate of 10°C min^{-1} and subsequently held it at 126.5°C for 120 min.

MFI measurements were conducted with a Tinius-Olsen Model MP993 Extrusion Plastometer according to ASTM D1238, using the 2.16 kg/190°C setup. A manual mode was used, in which a weighing specimen was cut every 360 s. Further melt rheology characterization was performed under oscillatory shear using a TA Instruments RSA 3 in shear-sandwich mode. Specimens with dimensions 12.7 × 16.0 × 0.5 mm^3 were prepared from compression-molded sheets. A frequency sweep of 0.01– 630 rad s^{-1} at 1% strain was programmed in a 170°C, dry air environment.

Macroscopic morphology analysis of samples was conducted on direct, transmission-mode optical microscope images taken using a Leica DM2700 M microscope. The spherulitic structure of the rHDPE samples were examined with a Leitz Wetzlar SM-LUX polarized optical microscope fitted with a Nikon Coolpix 900 digital camera. For both microscope studies, the specimens were prepared by compression molding the materials into <0.5-mm thick films in a Carver Model C Laboratory Press operating at 200°C.

Wide-angle X-ray diffraction (XRD) was conducted on the compression molded sheets using a PANalytical X'Pert Pro Multi-Purpose Diffractometer system with Cu Kα monochromatic rays generated at 45 kV and 40 mA. The detector was set to scan between $2\theta = 5°$ and 80° at 0.3° steps. Small-angle X-ray scattering (SAXS) measurements were conducted in Richard A. Register's Laboratory at Princeton University, whose system comprises a PANalytical PW3030 generator with Cu Kα rays at 40 kV and 30 mA, an Anton Paar compact Kratky camera, an MBraun OED-50M position sensitive detector, and a hotstage built in-house. The raw data were desmeared, corrected for empty beam scattering, normalized for sample thickness and transmittance, and calibrated with a polyethylene standard.

RESULTS AND DISCUSSION

Processing Conditions and Output

As seen in Figure 1, the contrastive processing methods expose rHDPE samples to different temperature, shearing, mixing, and pressure profiles, which results in varying product output forms and conditions.* Table I summarizes the important differences

*Single screw extrusion (SSE), another common industrial processing method for recycling plastics, was originally considered to be part of this comparative study but is omitted from the scope of the paper. Preliminary inspection and testing of rHDPE specimens made via SSE (Killion KLB-075, $D = 19$ mm, $L/D = 24$) indicated that the product consistency, MFI value, and mechanical performance are similar to, or worse than, TSE-processed specimens. As it is understood that SSE processing does not impart rigorous mechanical stress on the material in the melt, (Ref. 15) including it in the study would not have provided additional insights.

Table I. Processing Summary

Samples	Equipment power usage (kW)	Output (or as-received) form	Product uniformity	MFI[a] @ 190°C, 2.16 kg (g/10 min)
Unprocessed	0.0	(Flakes)	Low	0.66 ± 0.05
TSE	2.3	Strands/pellets	Medium	0.38 ± 0.01
SSSP-L	3.0	Powder	Medium	0.75 ± 0.01
SSSP-H	4.5	Powder	High	0.96 ± 0.03
SSME-L	4.2	Strands/pellets	High	0.50 ± 0.02
SSME-H	4.3	Strands/pellets	High	0.53 ± 0.01

[a] Values are expressed as arithmetic mean ± 1 standard deviation.

in the ways the specimens were produced. Equipment power usage, which was measured by a watt-hour meter in the laboratory, represents the electrical power required at steady-state production, and encompasses motor, heater and chiller loads as well as consumption by computing and controls. Most of the power used in the TSE operation went into heating the barrels. In contrast, SSSP runs required not only significant energy from the chiller to ensure low processing temperatures, but also higher motor load as compared to TSE; higher power is required because the rotating screws continuously fragment and fuse solid materials, rather than mix and knead molten materials. It was expected that the SSSP-H screw design would require higher motor load compared to its mild screw design analog. One may also expect SSME processing to require the most energy, for both chilling and heating the barrels and for the torque to process materials through both zones. The results, however, indicate that the energy cost for SSME runs is negligibly different or even lower than that of SSSP-H; this is most likely because SSME runs essentially have the same harsh screw elements as SSSP-H, and the chilling and heating duties in SSME are for shorter zone lengths compared to SSSP and TSE runs, respectively.

The output of rHDPE samples comes in three formats, as previously mentioned; they are summarized in Table I. As-received milk jug material had been prepared into flakes with lateral dimensions varying from 3 to 8 mm using an industrial granulator. TSE takes these irregular size flakes and produces molten strands, which are subsequently cooled and pelletized into consistently sized pieces. In contrast, SSSP processes the flake material in a chilled environment and produces materials in the form of coarse or fine powder. Despite SSSP's past successes in synthesizing a wide range of polymer-based blends and composites,[47–52] its powder product nature has prevented the relevant industries' adoption of the technology. Indeed, considerations for the ease of transportation and further processing/shaping as well as health and safety lead to a consensus that pellets are the industrial standard and preference. SSME was developed to specifically avoid the powder output by incorporating a short melt extrusion after solid-state pulverization in the same instrument.[53] As seen in Table I, SSME was able to produce molten extrudate samples of rHDPE, suitable for pelletization, just like TSE.

When the process outputs were shaped into various test specimens via compression-molding or injection-molding and inspected visually, there were distinct differences in the general consistency and color uniformity, as summarized in Table I. As discussed in the Materials Section, rHDPE samples contained trace amounts of paper, pigments, and other polymers that were not completely removed during the recycling process. These impurities are the typical causes of color streaks and inconsistent surface appearances in the specimens. The optical microscope images in Figure 2 depict the varying levels and degrees of these non-uniformities. A compression-molded specimen of unprocessed, as-received milk jug flakes exhibited numerous imperfections in the form of strips and islands [Figure 2(a)], which had been reduced to sizes on the order of millimeters via an earlier granulating step. A specimen molded from TSE-processed rHDPE also shows similar types of impurities, albeit in a lower concentration [Figure 2(b)]; rigorous melt mixing at

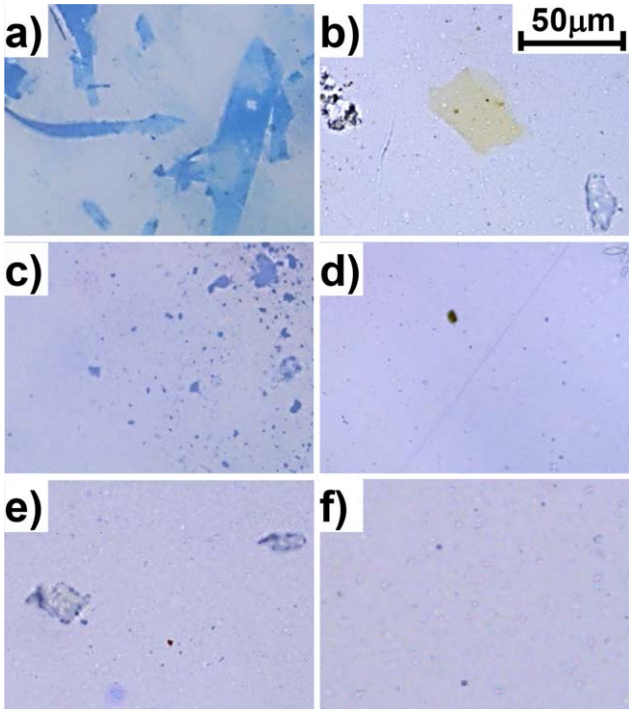

Figure 2. Optical microscope images of 0.5-mm thick compression-molded rHDPE sheets from: (a) Unprocessed, (b) TSE, (c) SSSP-L, (d) SSSP-H, (e) SSME-L, and (f) SSME-H specimens. The scale bar applies to all images. [Color figure can be viewed in the online issue, which is available at wileyonlinelibrary.com.]

temperatures above 200°C led to co-melting and subsequent distribution of LDPE and PP impurities within the HDPE matrix. The samples processed via SSSP and SSME had been subjected to a much harsher solid-state compounding process, where considerable fragmentation and fusion of the materials occurred. Therefore, the corresponding microscope images in Figure 2(c–f) exhibit reduced amounts and sizes of visible impurities. In both SSSP and SSME, a harsher screw setting leads to compression-molded specimens with very little, if any, visible impurity particles on the order of sub-millimeters. The high levels of impurity size reduction and homogeneous mixing observed in SSSP-H and SSME-H specimens are expected to translate and sustain in subsequent processing, such as injection molding.

MFI is employed to supplement the above visual inspection results, as a metric to compare the physical consistency and processability of the six rHDPE samples. Given that the MFI value of a blow-molding grade vHDPE sample is 0.8 g/10min at 190°C and 2.16 kg, the MFI value of the unprocessed rHDPE in Table I is reasonable. The rHDPE samples that were processed via SSSP exhibited significantly increased MFI values, indicating a less viscous, liquid-like consistency if they were to be processed further via extrusion and other melt-based techniques. On the other hand, the rHDPE samples that were processed via TSE and SSME exhibited significantly reduced MFI values, indicating a more viscous melt consistency in the case of further processing. The reason why the SSME-processed specimens experienced only moderate reductions in MFI, compared to the TSE specimen, is because SSME process is part SSSP and part TSE; the MFI shifts in SSME-specimens can be described as an additive response from the two parts. Nonetheless, the bipolar direction of MFI values is intriguing and will be discussed further in a later section. One phenomenon worth noting here is that the variation of the MFI data (insofar as the standard deviation values, with respect to the average MFI values) has narrowed following processing, which implies that batch-to-batch/over-time variations in process characteristics (e.g., melt strength, extruder/molder torque) and product specifications (e.g., color, physical properties) can be controlled when these processing techniques are employed. Specifically, running the rHDPE flakes through SSME-H reduces the variation of average MFI values fourfold, from 8% (s.d. of 0.05 for an average of 0.66) to 2% (s.d. of 0.01 for an average of 0.53).

Mechanical Performance

The results of the room-temperature tensile test are summarized in Table II; for a better visual comparison of mechanical behaviors, Figure 3 plots a representative stress-strain curve of each specimen, along with that of a control, commercial vHDPE sample. Qualitative data comparison in Figure 3 suggests that the stress-strain behaviors of the samples are essentially identical through the yield point. In fact, as seen in Table II, the Young's modulus and yield strength values of the six rHDPE samples were found to be the same, within error, and consistent with the measured values for the control vHDPE specimen, 1.02 GPa and 30 MPa, respectively. Despite varying levels of possible impurities, and even though some of the processing methods in this study expose the post-consumer HDPE to high degrees of shear, compression, and mixing, the two important room temperature mechanical properties remain essentially unaffected; this conclusion aligns with some of the previous findings on processing of (r)HDPEs.[13,15–17,46]

The most intriguing observation from Table II and Figure 3 is the ductility improvement when rHDPE is processed in the extruder-based techniques. The specimens molded from unprocessed rHDPE exhibit an impractically low strain at break, which is a major drawback generally associated with impure, recycled plastics. Processing the same material via TSE or SSSP-H enhances its strain at break by nearly 6- and 7-fold, respectively, effectively "recovering" the expected ductility of HDPE to an extent. The SSME processes further enhance the rHDPE strain at break by more than 11-fold, to ~700% strain at break that vHDPE sample exhibits, as seen in Figure 3. The improvements in tensile ductility directly translate to equivalent levels of enhancement in tensile toughness (taken as the area under the stress-strain curve), because the moduli and strengths are the same across the series. Qualitative differences in the areas under curve can be discerned in Figure 3, while the calculated tensile toughness values are recorded in Table II. In addition to tensile property characterization, the impact toughness of injection molded specimens was also assessed. The unnotched Izod impact resistance results in Table II indicate that all types of processing except for SSSP-L enhanced the impact resistance of rHDPE to varying extents, but all near or above that of the vHDPE control (measured as 850 J m^{-1}). The SSME-H process had the most significant improvement, where the impact resistance nearly doubled compared to the unprocessed case.

These substantial improvements in ductility and toughness of SSME-processed and, to a lesser extent, SSSP-processed rHDPE, to values near or above those of typical blow-molding grade vHDPE are significant from the standpoint of plastics processing and manufacturing. The results refute the common impression that impure post-consumer plastics have inferior mechanical properties, and provide an opportunity for rHDPE to broaden its applicability. Khait *et al.* have previously reported on a 30% ductility increase in SSSP-processed HDPE, and a larger, sixfold increase in SSSP-processed LLDPE,[43] however, to our knowledge, there are no reports of improvements in the tensile and impact toughnesses of post-consumer HDPE as large as our results. It is also important to note, based on the standard deviation values (relative to the average values) in Table II, that the variability of mechanical properties become narrower with most processing techniques, with SSME-H providing the most consistent performance. This observation is in line with the tightening of output color and melt flow variability discussed earlier, and is a confirmation that SSME-H processing can yield reproducible, reliable rHDPE products with minimal batch-to-batch and over-time variation.

Even though it is intuitive to link the toughness improvements and tightened processing and product specifications in SSME-H and other processed samples to the size reduction and fine distribution of label and lid impurities as seen in Figure 2, we do not believe that the physical, macroscopic impurity manipulation is the sole reason for such drastic improvements. We have

Table II. Mechanical Properties of rHDPE Specimens

	Uniaxial tensile test				Impact test
Samples	Young's modulus (GPa)	Yield strength (MPa)	Strain at break (mm mm^{-1})	Tensile toughness (J m^{-3})	Impact resistance (J m^{-1})
Unprocessed	1.13 ± 0.06	29 ± 2	0.5 ± 0.5	10 ± 10	680 ± 80
TSE	1.15 ± 0.04	31 ± 1	2.8 ± 1.5	59 ± 31	840 ± 150
SSSP-L	1.07 ± 0.09	29 ± 2	0.7 ± 1.0	14 ± 20	520 ± 110
SSSP-H	1.10 ± 0.07	31 ± 2	3.6 ± 2.5	74 ± 52	1080 ± 80
SSME-L	1.08 ± 0.08	29 ± 1	5.9 ± 2.0	120 ± 42	920 ± 60
SSME-H	1.11 ± 0.05	30 ± 1	7.3 ± 0.7	146 ± 18	1300 ± 60

Values are expressed as arithmetic mean ± 1 standard deviation.

conducted a follow-up analysis of mechanical properties on an unprocessed rHDPE batch from which all non-HDPE particulates had been manually removed; the tensile properties of this manually purified, unprocessed rHDPE sample were equivalent to the unimpressive properties of as-received unprocessed rHDPE, within error.

Morphology Characterization

To elucidate the processing-structure-property relationship in rHDPE, we examined the effects of processing on ethylene crystallite morphology; the results of detailed calorimetry experiments are displayed in Table III. Percent crystallinity of rHDPE, measured during a 10°C heating ramp of molded specimens, suffered a slight decrease when processed. At the same time, as evidenced by the decrease in onset crystallization temperature at 10°C cooling ramp, as well as a more pronounced difference in isothermal crystallization half-time, the ethylene crystallization rate slowed when rHDPE is processed by any of the extruder-based methods studied. While the magnitudes of some of these changes are not very large, the general trend is atypical of semi-crystalline polymers processed via SSSP or SSME; a previous report of processing virgin PP in SSSP had its isothermal crystallization half-time reduce by twofold, as a result of increased chain mobility.[45] Table III further reveals that the onset melting temperatures of the processed samples were higher than the unprocessed, implying that the dimensions of the crystallites developed in the processed samples are larger.[54]

X-ray scattering, in both wide- and small-angle settings, was employed to probe the morphology of fundamental ethylene crystals on unit-cell and crystalline lamellar levels, respectively. XRD patterns of the unprocessed and five processed rHDPE samples all had the same characteristic peaks [e.g., at $2\theta = 21.3°$ for (110) and $2\theta = 23.7°$ for (200)] corresponding to the ethylene unit cell structure,[5] with indiscernible differences in their features such as peak positions and widths at half maximum. These results confirm little to no disruption of the chain arrangements in ethylene crystals upon TSE, SSSP, or SSME processing of rHDPE. On the other hand, Figure 4 shows that the five processed samples exhibited SAXS spectra with lower peak positions, q^*, in reference to that of the unprocessed rHDPE sample. While the SSSP specimens experienced only a negligible shift, both TSE and SSME samples had a more pronounced shift toward lower q^*, by about 20%. A reduction in q^* in SAXS characterization corresponds to an increase in lamellar spacing according to Bragg's law. Quantitatively, average lamellae thickness, L, of the samples can be calculated using a first-order simple model, $L = (2\pi/q^*)$ (degree of crystallinity). Using the crystallinity data in Table III, the average lamellae thicknesses of TSE- and SSME-processed samples were calculated to be 20 and 19 nm, respectively, which are larger than the calculated L of 18 nm for the unprocessed sample. This comparison confirms an earlier observation that the rHDPE crystallites processed via TSE and SSME are thicker than those in the unprocessed sample.

As a higher hierarchical-level morphology investigation, POM was conducted to probe the spherulite structure of the molded rHDPE specimens. The comparative images in Figure 5 show that the unprocessed rHDPE spherulite pattern remains relatively unchanged with TSE or SSSP-L processing, but becomes visibly larger upon SSSP-H and both types of SSME processing; SSME-H specimen, Figure 5(f), exhibited the largest spherulite elements relative to other specimens, on the order of 5–7 μm, which matched those found in the vHDPE control sample in a follow-up POM imaging. In effect, based on comprehensive DSC, SAXS,

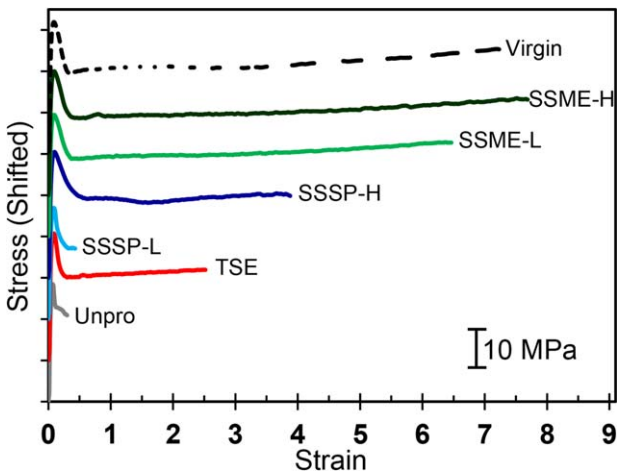

Figure 3. Representative uniaxial tensile test results of the samples. The stress-strain curves are shifted by 10 MPa. The top curve is commercial virgin HDPE used as a reference. [Color figure can be viewed in the online issue, which is available at wileyonlinelibrary.com.]

Table III. Thermal Properties of rHDPE Specimens

Samples	Percent crystallinity, @ +10°C/min (%)	Onset crystallization temperature, @ −10°C min^{-1} (°C)	Crystallization half-time, @ 126.5°C (min)	Onset melting temperature, @ +10°C min^{-1} (°C)
Unprocessed	73.4	123	7.5	124
TSE	68.9	123	8.1	127
SSSP-L	62.5	123	8.1	128
SSSP-H	68.6	122	11.0	127
SSME-L	68.3	121	13.4	127
SSME-H	65.2	121	13.1	127

and POM results, we confirm that processing rHDPE with high solid-state shearing (SSME-H in particular but also SSSP-H and SSME-L) leads to ethylene crystallite morphology with lower crystalline fraction, lower crystallization kinetics, and thicker crystalline lamellae and enlarged spherulites, compared to the as-received, unprocessed state. In the context of the observed improvement in ductility and toughness of rHDPE, these morphological accounts are perhaps unexpected, because numerous reports in the literature consistently claim that thicker crystalline lamellae and larger spherulites structures in semi-crystalline polymers lead to reduction in strain at break and impact strength.[55–57] However, these earlier studies controlled the spherulites size via simple means such as cooling rate and degree of polymerization, and their relation of sample brittleness to spherulite size may be oversimplified. The fracture mechanism of semi-crystalline polymers can be more complex, especially when changes in molecular architecture are involved.[58–60] Therefore, understanding why our SSSP- and SSME-processed rHDPE samples have improved ductility and toughness while exhibiting larger crystallite/spherulite features in their morphology, requires a close look at the polymer chain structure.

Molecular Architecture Origins

We revisit the MFI results in Table I, and complement the analysis with oscillatory shear rheology characterization. First, a noticeable rise in MFI, by as large as by 45%, is observed when rHDPE is processed via SSSP. In Figure 6, the shear storage modulus (G') and shear loss modulus (G'') curves of the two SSSP specimens almost coincide, and they essentially follow the respective curves of the unprocessed specimen at slightly lower moduli. Additionally, the G'-G'' crossover points for the two SSSP specimens remain fairly unchanged from that for the unprocessed specimen. Thus the SSSP-processed rHDPE samples are envisioned to have undergone simple chain scission, as proposed by previous work.[44,45,48] Repeated fragmentation of the material by shear and compressive forces creates macroradicals, which combines with surrounding macroradicals or oxygen molecules; because the process occurs in the solid state at a low temperature, complex molecular events like radical transfers are not likely, and molecular weight reduction prevails. Contrary to the above SSSP-process scenario is the lowering of the MFI values upon TSE- and SSME-processing, as shown in Table I. The rheology data in Figure 6 indicate that the G'-G'' crossover points are at progressively lower frequency and modulus values for SSME-H, SSME-L and TSE. Such shifts in oscillatory shear data have previously been observed in processed (r)HDPEs, and attributed to preferential side-chain branching or crosslinking over chain scission.[11–13,21,46] Melt-kneading in a twin screw extruder is a heavily thermomechanical process, and rigorous mixing in high temperature-viscous melt provides the opportunities for degradation of ethylene chains with active chain interactions and complex radical transfers. While further molecular characterization to probe the details of side-chain branching may be useful, we believe that branching provided sufficient changes in the melt flow behavior and crystalline/amorphous morphology, and in turn in the tensile and impact fracture toughness of the samples. It is important to note the minimally affected tensile stiffness and strength data in Table II; the frequency and degree of branching are not at the level where the fundamental mechanics of the samples deteriorate, as also confirmed in previous studies.[45,46]

When the chains of a semicrystalline polymer with sufficient driving force crystallize from the melt, irregularities within, such as branch points, as well as outside, like impurity materials, are likely to be excluded from the growing crystallites.[61]

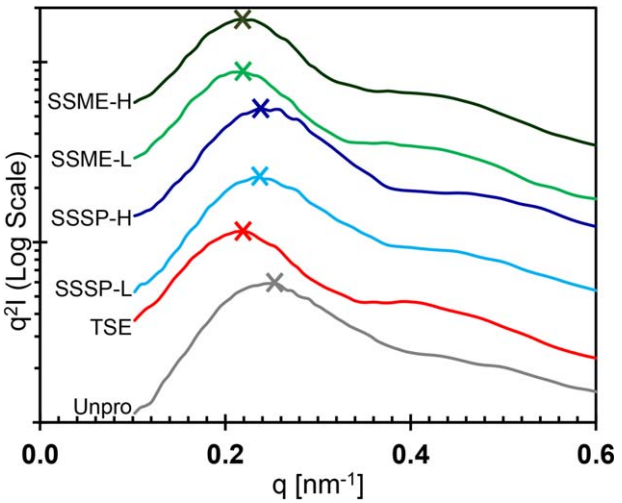

Figure 4. SAXS profiles of unprocessed and processed rHDPE samples. The abscissa is the momentum transfer vector $q = (4\pi/\lambda)\sin\theta$, where λ is the Cu Kα X-ray wavelength (0.1542 nm) and θ is half the scattering angle. The ordinate is the Lorentz-corrected intensity. The curves are shifted vertically with a constant multiplier for clarity, and the crosshairs signify peaks. [Color figure can be viewed in the online issue, which is available at wileyonlinelibrary.com.]

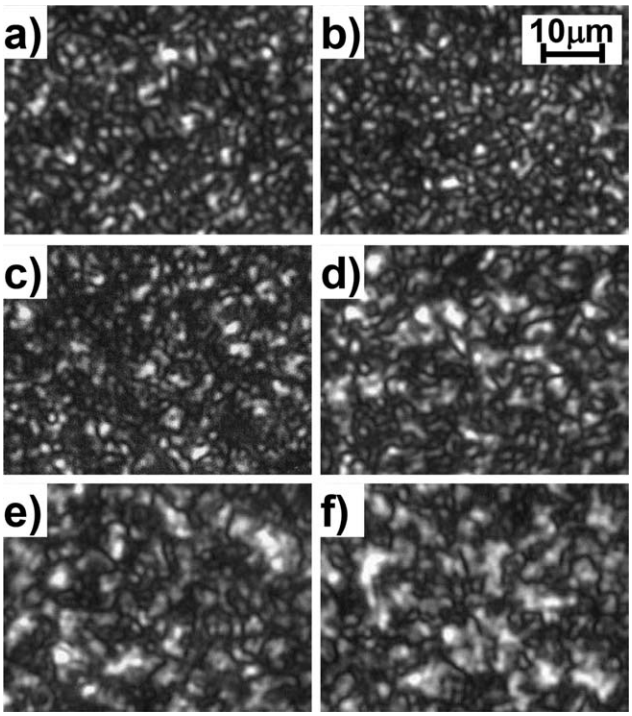

Figure 5. Polarized optical microscope images of thinly compression-molded rHDPE sheets from: (a) Unprocessed, (b) TSE, (c) SSSP-L, (d) SSSP-H, (e) SSME-L, and (f) SSME-H specimens. The scale bar applies to all images.

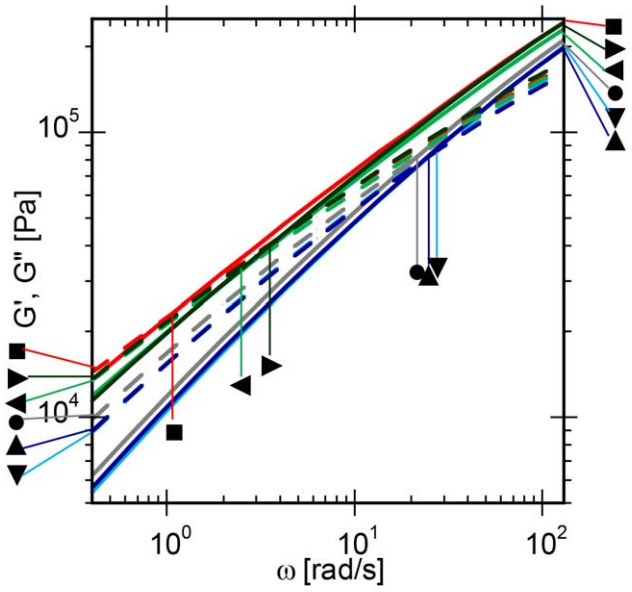

Figure 6. G' (solid) and G'' (dashed) as a function of angular frequency from the oscillatory shear rheology measurements. The markers, (●) Unprocessed, (■) TSE, (▼) SSSP-L, (▲) SSSP-H (◀) SSME-L (▶) SSME-H point to the corresponding G'' curves from the left y axis, point to the G' curves from the right y axis, and point at the G'-G'' crossover points inside the graph. The relative positions, both in x- and y-coordinates, of the crossover point markers reflect the relative positions of the actual crossover points. [Color figure can be viewed in the online issue, which is available at wileyonlinelibrary.com.]

Bubeck and Baker found that short chain branch length and concentration have a monotonic relation with resulting spherulite size.[62] In the present investigation, rHDPE was processed through various extents to which the impurities were dispersed and branch points were created, and consequently, the nature of crystallization was modified; the calorimetry results corroborate this argument as the rigorously processed samples, such as SSME-H, exhibited not only lower crystallinity and slower rate of crystallization, but also larger spherulites stemming from lower number of nucleation sites. However, it is equally important to consider the effect of the excluded party, i.e. the branch points and/or impurities along with the remainder of ethylene chains, upon the fracture behavior of the polymer. Previous reports in the literature emphasize that branched tie molecules[63] contribute to robust inter-spherulite and inter-lamellar links, and control the tensile and impact toughness of polyethylene.[64–66] In our investigation, the extruder-based processing methods created an effective molecular architecture and provided a homogeneous amorphous region with even distribution of impurities, resulting in greater links between the crystallites and spherulites.

To recapitulate our processing-structure-property analyses, both TSE and SSME relied on rigorous kneading in the viscous melt to impart an appreciable level of branching in the molecular architecture, but SSME showed larger enhancements in ductility and toughness. Both SSSP and SSME applied high shear and compression to pulverize impurities and disperse them throughout the materials, but SSME again exhibited larger enhancements in ductility and toughness. Neither TSE nor SSSP alone provided the level of mechanical property increase that SSME-H achieved. SSME exercises an ideal combination of chain scission, chain branching, impurity distribution, and material homogenization, by subjecting the material to solid-state shear pulverization immediately followed by rigorous melt mixing. It is indeed attractive that SSME combines the positive effects of TSE and SSSP processing and produces a reliable, non-powder form of rHDPE with improved ductility and toughness with minimal sacrifice to the crystalline structure and almost no deterioration of other physical properties. For tailoring the product to desired specifications (e.g., MFI) and applications, SSME can be tuned easily through processing parameters such as screw design, screw speed, and solid-state/melt zone lengths. Optimization studies to scale the SSME process to industrial-level production are currently underway.

CONCLUSIONS

Twin screw extruder-based processing techniques with varying temperature and screw profiles were explored as a means to improve the spec consistency and overall properties of recycled plastics. Processing post-consumer milk jug rHDPE in TSE, SSSP, and SSME without additives or processing aids yielded products with consistent appearance and performance, and marked increase in tensile ductility and impact toughness.

Our processing-structure-property analyses indicate that a series of physical and chemical modifications of rHDPE material is attributed to the enhanced properties. Solid-state shearing,

applied in SSSP and part of SSME, provides solid-state fragmentation and mixing to mechanically reduce and disperse the impurities, and chemically scission ethylene chains. Melt-state kneading, applied in TSE and part of SSME, uses high temperature and viscous mixing to intimately blend and distribute polymer molecules with impurities and imperfections, and induce side-chain branching of polymer chains. In effect, SSME performs both sets of desired modifications at appropriate levels, and in turn imparts a semi-crystalline polymer morphology that is uniform and well-connected.

SSME processing, especially with a harsh screw configuration, combines the positive mechanochemical effects and practical advantages of SSSP and TSE, to stand out as a synergistic extruder-based technology for promoting wider industrial applications of post-consumer plastics. In combating growing waste concerns, SSME is indeed an industrially scalable, environmentally friendly, and sustainable processing technique with a vision of upcycling plastics.

ACKNOWLEDGMENTS

The extruder equipment, funded by National Science Foundation Major Research Instrumentation Grant, CMMI-0820993 (any opinions, findings, and conclusions or recommendations expressed in this material are those of the authors and do not necessarily reflect the views of NSF), is under continual technical support by KraussMaffei Berstorff Corporation (Florence, KY, U.S.A.). The authors are grateful to Mr. Patrick Kelley of Waste Not Technologies, LLC (Saylorsburg, PA) for providing materials as well as valuable discussions and feedback. The authors are indebted to Prof. Richard A. Register and Mr. William D. Mulhearn of Princeton University for the SAXS data. Lastly, Bucknell University provided personnel support: Diane L. Hymas Undergraduate Research Fund in Engineering (EVM); Program for Undergraduate Research (SHJ); and Engineering Dean's Fellowship (KW).

REFERENCES

1. La Mantia, F. P. Handbook of Plastics Recycling; Rapra Technology: Shawbury UK, **2002**.
2. Vilaplana, F.; Karlsson, S. *Macromol. Mater. Eng.* **2008**, *293*, 274.
3. Al-Salem, S. M.; Lettieri, P.; Baeyens, J. *Waste Manage.* **2009**, *29*, 2625.
4. Production and Sales Data by Resin, 2014 vs. 2013; American Chemistry Council: Washington DC, **2015**.
5. Peacock, A. J. Handbook of Polyethylene: Structures, Properties, and Applications; Marcel Dekker: New York, NY, **2000**.
6. Vasile, C.; Pascu, M. Practical Guide to Polyethylene; Rapra Technology: Shrewsbury UK, **2005**.
7. Waste Reduction Model Version 13; United States Environmental Protection Agency: Washington DC, **2015**.
8. 2013 National Post-Consumer Plastics Bottle Recycling Report; American Chemistry Council: Washington DC, **2014**.
9. McDonough, W.; Braungart, M. Cradle to Cradle: Remaking the Way We Make Things; North Point Press: New York, NY, **2002**.
10. Camacho, W.; Karlsson, S. *J. Appl. Polym. Sci.* **2002**, *85*, 321.
11. Cruz, S. A.; Zanin, M. *Polym. Degrad. Stab.* **2003**, *80*, 31.
12. Kealy, T. *J. Appl. Polym. Sci.* **2009**, *112*, 639.
13. Oblak, P.; Gonzalez-Gutierrez, J.; Zupancic, B.; Aulova, A.; Emri, I. *Polym. Degrad. Stab.* **2015**, *114*, 133.
14. Zahavich, A. T. P.; Latto, B.; Takacs, E.; Vlachopoulos, J. *Adv. Polym. Technol.* **1997**, *16*, 11.
15. Loultcheva, M. K.; Proietto, M.; Jilov, N.; La Mantia, F. P. *Polym. Degrad. Stab.* **1997**, *57*, 77.
16. Mendes, A. A.; Cunha, A. M.; Bernardo, C. A. *Polym. Degrad. Stab.* **2011**, *96*, 1125.
17. Takatori, E.; Shimura, T.; Adachi, T.; Yao, S.; Shindoh, Y. *Nihon. Reoroji. Gakk.* **2014**, *42*, 45.
18. Casey, D.; McNally, C.; Gibney, A.; Gilchrist, M. D. *Resour. Conserv. Recy.* **2008**, *52*, 1167.
19. Siddique, R.; Khatib, J.; Kaur, I. *Waste Manage.* **2008**, *28*, 1835.
20. Sobhan, K.; Mashnad, M. *J. Mater. Civ. Eng.* **2002**, *14*, 177.
21. Pattanakul, C.; Selke, S.; Lai, C.; Miltz, J. *J. Appl. Polym. Sci.* **1991**, *43*, 2147.
22. Cruz, S. A.; Zanin, M. *J. Appl. Polym. Sci.* **2004**, *91*, 1730.
23. Miller, P.; Sbarski, I.; Kosior, E.; Masood, S.; Iovenitti, P. *J. Appl. Polym. Sci.* **2001**, *82*, 3505.
24. Albano, C.; Sanchez, G. *Polym. Eng. Sci.* **1999**, *39*, 1456.
25. Kukaleva, N.; Simon, G. P.; Kosior, E. *Polym. Eng. Sci.* **2003**, *43*, 26.
26. Li, Z.; Gao, H.; Wang, Q. *J. Appl. Polym. Sci* **2012**, *124*, 5247.
27. Cao, X. V.; Ismail, H.; Rashid, A. A.; Takeichi, T.; Thao, V. H. *Bioresources* **2011**, *6*, 3260.
28. Favaro, S. L.; Ganzerli, T. A.; de Carvalho Neto, A. G. V.; da Silva, O. R. R. F.; Radovanovic, E. E. *Polym. Lett.* **2010**, *4*, 465.
29. Kamdem, D. P.; Jiang, H. H.; Cui, W. N.; Freed, J.; Matuana, L. M. *Compos. Part A Appl. S.* **2004**, *35*, 347.
30. Lu, N.; Oza, S. *Compos. Part B Eng.* **2013**, *45*, 1651.
31. Nourbakhsh, A.; Ashori, A. *J. Compos. Mater.* **2009**, *43*, 877.
32. Atikler, U.; Basalp, D.; Tihminlioglu, F. *J. Appl. Polym. Sci.* **2006**, *102*, 4460.
33. Chen, R. S.; Ahmad, S.; Gan, S.; Ab Ghani, M. H.; Salleh, M. N. *J. Appl. Polym. Sci.* **2015**, *132*, 42287.
34. Lei, Y.; Wu, Q.; Clemons, C. M. *J. Appl. Polym. Sci.* **2007**, *103*, 3056.
35. Colom, X.; Canavate, J.; Carrillo, F.; Sunol, J. J. *J. Appl. Polym. Sci.* **2009**, *112*, 1882.
36. Grigoryeva, O. P.; Fainleib, A. M.; Tolstov, A. L.; Starostenko, O. M.; Lievana, E.; Karger-Kocsis, J. *J. Appl. Polym. Sci.* **2005**, *95*, 659.
37. Shojaei, A.; Yousefian, H.; Saharkhiz, S. *J. Appl. Polym. Sci.* **2007**, *104*, 1.

38. Kartalis, C. N.; Papaspyrides, C. D.; Pfaendner, R.; Hoffmann, K.; Herbst, H. *J. Appl. Polym. Sci.* **1999**, *73*, 1775.
39. Madi, N. K. *Mater. Des.* **2013**, *46*, 435.
40. Abad, M. J.; Ares, A.; Barral, L.; Cano, J.; Diez, F. J.; Garcia-Garabal, S.; Lopez, J.; Ramirez, C. *J. Appl. Polym. Sci.* **2004**, *92*, 3910.
41. Pawlak, A.; Morawiec, J.; Pazzagli, F.; Pracella, M.; Galeski, A. *J. Appl. Polym. Sci.* **2002**, *86*, 1473.
42. Elmaghor, F.; Zhang, L. Y.; Li, H. Q. *J. Appl. Polym. Sci.* **2003**, *88*, 2756.
43. Khait, K.; Torkelson, J. M. *Polym. Plast. Technol.* **1999**, *38*, 445.
44. Khait, K.; Carr, S. H.; Mack, M. H. Solid-State Shear Pulverization: A New Polymer Processing and Powder Technology; Technomic: Lancaster PA, **2001**.
45. Brunner, P. J.; Clark, J. T.; Torkelson, J. M.; Wakabayashi, K. *Polym. Eng. Sci.* **2012**, *52*, 1555.
46. Ganglani, M.; Torkelson, J. M.; Carr, S. H.; Khait, K. *J. Appl. Polym. Sci.* **2001**, *80*, 671.
47. Furgiuele, N.; Lebovitz, A. H.; Khait, K.; Torkelson, J. M. *Polym. Eng. Sci.* **2000**, *40*, 1447.
48. Lebovitz, A. H.; Khait, K.; Torkelson, J. M. *Macromolecules* **2002**, *35*, 8672.
49. Iyer, K. A.; Torkelson, J. M. *Compos. Sci. Technol.* **2014**, *102*, 152.
50. Iyer, K. A.; Torkelson, J. M. *Polym. Compos.* **2013**, *34*, 1211.
51. Masuda, J.; Torkelson, J. M. *Macromolecules* **2008**, *41*, 5974.
52. Wakabayashi, K.; Pierre, C.; Dikin, D. A.; Ruoff, R. S.; Ramanathan, T.; Brinson, L. C.; Torkelson, J. M. *Macromolecules* **2008**, *41*, 1905.
53. Whittington, A. M.; Brouse, S. M.; Malusis, M. A.; Wakabayashi, K. *Adv. Polym. Technol.* **2013**, *32*, 21334.
54. Wunderlich, B. Macromolecular Physics. 3: Crystal Melting; Academic Press: New York, NY, **1973**.
55. Ohlberg, S. M.; Roth, J.; Raff, R. A. V. *J. Appl. Polym. Sci.* **1959**, *1*, 114.
56. Salazar, A.; Rico, A.; Rodriguez, S.; Navarro, J. M.; Rodriguez, J. *Polym. Eng. Sci.* **2012**, *52*, 805.
57. Perkins, W. G. *Polym. Eng. Sci.* **1999**, *39*, 2445.
58. Schultz, J. M. *Polym. Eng. Sci.* **1984**, *24*, 770.
59. Ouederni, M.; Phillips, P. J. *J. Polym. Sci. Polym. Phys.* **1995**, *33*, 1313.
60. Avella, M.; dell'Erba, R.; Martuscelli, E.; Ragosta, G. *Polymer* **1993**, *34*, 2951.
61. Keith, H. D.; Padden, F. J. *J. Appl. Phys.* **1964**, *35*, 1270.
62. Bubeck, R. A.; Baker, H. M. *Polymer* **1982**, *23*, 1680.
63. Keith, H. D.; Padden, F. J.; Vadimsky, R. G. *J. Polym. Sci.* **1966**, *4*, 267.*A2*
64. Gupta, P.; Wilkes, G. L.; Sukhadia, A. M.; Krishnaswamy, R. K.; Lamborn, M. J.; Wharry, S. M.; Tso, C. C.; DesLauriers, P. J.; Mansfield, T.; Beyer, F. L. *Polymer* **2005**, *46*, 8819.
65. Liu, T. M.; Baker, W. E. *Polym. Eng. Sci.* **1992**, *32*, 944.
66. Kennedy, M. A.; Peacock, A. J.; Failla, M. D.; Lucas, J. C.; Mandelkern, L. *Macromolecules* **1995**, *28*, 1407.